Reprinted from:
BIOPHYSICS OF HAIR-CELL SENSORY SYSTEMS,
H. Duifhuis, J. W. Horst, P. van Dijk, and S. M. van Netten, Eds.
(World Scientific, Singapore, 1993), pp. 272-279

Analysis of dynamical motion of sensory cells in the Organ of Corti using the spectrogram

M. C. Teich[1], C. Heneghan[1], S. M. Khanna[2], Å. Flock[3], L. Brundin[3], and M. Ulfendahl[3]

[1] *Departments of Electrical Engineering and Applied Physics, Columbia University*
500 West 120th Street, New York, NY 10027, U.S.A.
[2] *Fowler Memorial Laboratory, Department of Otolaryngology, College of Physicians & Surgeons, Columbia University*
630 West 168th Street, New York, NY 10032, U.S.A.
[3] *Department of Physiology II, Karolinska Institutet*
S-10401 Stockholm, Sweden

1 Introduction

Although most studies of nonlinearity in the cochlea have focused on the nonlinear response of the basilar membrane (Rhode, 1971; LePage and Johnstone, 1980; Sellick *et al.*, 1982; Robles *et al.*, 1989), we have previously used laser interferometry (ITER, 1989) to observe unusual nonlinear dynamical motions (Teich *et al.*, 1989) of outer hair cells and Hensen's cells in the apical turn of the guinea-pig temporal-bone preparation (Ulfendahl *et al.*, 1989).

A unique feature of nonlinear dynamics is a time response whose character depends on stimulus level. To provide an acoustic stimulus with variable level, we have made use of a slowly varying amplitude-modulated (AM) tone. The time responses of sensory cells (velocity versus time) in the presence of such stimuli were examined using spectrogram analysis. This technique is particularly well suited to revealing time variations in the spectrum of a vibratory response as the stimulus level changes. We also examined the frequency-dependent nature of the nonlinear dynamical motion by altering the carrier frequency of the AM stimulus.

2 Experimental Procedure

The modulation frequency of the AM stimulus was fixed at 2.44 Hz, and 100% modulation was used at all times. The carrier frequency of the AM stimulus was varied in 25 or 50 Hz steps from 25 Hz to 2000 Hz. A sampling rate of 5 kHz was used in recording the data. A probe microphone recorded the sound pressure level (SPL) at the tympanic membrane, simultaneously with cellular velocity measurements. In the temporal-bone preparation, the middle ear is fluid-filled, which introduces an acoustic intensity loss of approximately 35 dB (Franke *et al.*, 1992). All sound pressure levels

quoted in this paper are therefore reduced by 35 dB relative to the sound pressure level measured at the tympanic membrane (dB re 0.0002 dyne/cm^2).

3 Analysis Technique

A slowly varying AM tone was chosen since this stimulus allowed us to track the response of the cell at a single frequency (the carrier frequency) over a wide range of intensities. The spectrogram [the squared magnitude of the Short Time Fourier Transform ($STFT$)] allows us to trace the changes in the spectral response as a function of time.

The $STFT$ is the Fourier transform of a windowed time waveform (Oppenheim and Schafer, 1989). In the continuous domain, the $STFT$ is written as

$$STFT_x^g(t,f) = \int_{-\infty}^{\infty} [x(u)g^*(u-t)] \exp(-j2\pi f u)\, du, \tag{1}$$

where $x(t)$ represents the time waveform being analyzed, $g(t)$ represents a window function in time, t is the time variable, and f is the frequency variable. The Gaussian window [$g(t) = \exp(-t^2)$] is a good choice for $g(t)$ since it maximizes the available time and frequency resolution for this transform. A discrete version of this transform can be implemented using a summation approximation to Eq. 1:

$$STFT[n,k] = \sum_{m=0}^{L-1} x[n+m]w[m] \exp\left(\frac{-j2\pi mk}{N}\right), \quad 0 \le k \le N-1, \tag{2}$$

where L is the width of the time-window in number of samples, n is the discrete time index, k is the discrete frequency index, and $w[m]$ represents the Gaussian window sampled in the range $[-2,2]$. The value of N (which sets the number of discrete frequencies at which the $STFT$ is sampled in the frequency domain) was chosen equal to L. The spectrogram was not evaluated for all values of n; sampling at values of n that were multiples of 8 usually gave a sufficiently detailed picture of the spectrogram for our purposes.

Strictly speaking, the spectrogram is defined as the squared magnitude of the $STFT$ defined in Eq. 1, but we plot the magnitude of the $STFT$, since that allows both low- and high-magnitude spectral components to be represented in a more compact range. The spectrogram is presented in a 3D format. Time and frequency form the bottom plane, and the magnitude of the $STFT$ is represented on a linear axis in the third dimension. The magnitude of the $STFT$ is normalized so that its value can be interpreted in terms of the units of the input waveform (i.e., in spectrograms of velocity waveforms, the magnitude of the $STFT$ can be interpreted as velocity).

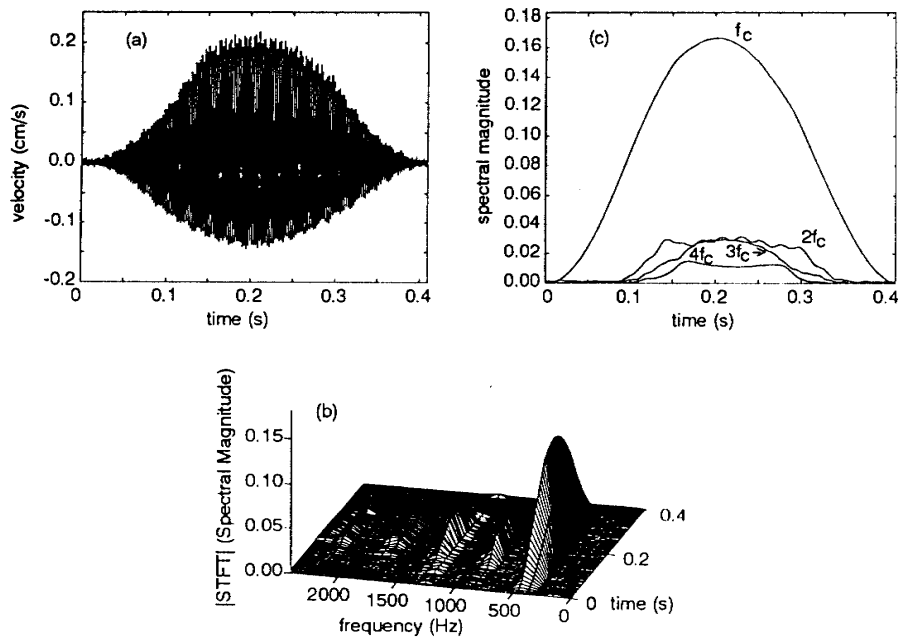

Figure 1: Velocity response of a second-row outer hair cell (0b081215.dt3) in the third turn of the guinea-pig temporal-bone preparation to an AM stimulus with a carrier frequency of 439 Hz (below CF) and a modulation frequency of 2.44 Hz. (*a*) Time waveform of the velocity response (in cm/s) of the cell. Note the asymmetry. (*b*) Spectrogram of the velocity response shown in (*a*). The x and y axes represent time (s) and frequency (Hz) respectively, and spectral magnitude is plotted on the z axis (unitless). The spectrogram shows components at the carrier frequency f_c, and at the four higher harmonic frequencies $2f_c$, $3f_c$, $4f_c$, and $5f_c$. For the central portion of the response, the third harmonic is nearly equal in magnitude to the second harmonic. (*c*) Time course of the four most significant spectral components in the velocity response ($f_c, 2f_c, 3f_c$, and $4f_c$) extracted directly from the spectrogram in (*b*), showing how the spectral magnitude of each harmonic component varies in time. The carrier frequency component follows the envelope of the modulation. However the component at $2f_c$ flattens near the center of the envelope and components appear at higher harmonics ($3f_c, 4f_c$, and $5f_c$).

4 Results

4.1 Response of an outer hair cell to an AM stimulus with a carrier frequency below its characteristic frequency

We report the response of an outer hair cell in the third turn of the guinea-pig cochlea. This cell has a characteristic frequency (CF) of approximately 700 Hz in its velocity

response to sinusoidal stimuli of constant intensity. Figure 1 shows the response when an AM tone with a carrier frequency $f_c = 439$ Hz (below CF) is applied to the cochlear preparation.

In Fig. 1(a), the observed velocity response to the AM stimulus is shown. The response does not precisely follow the input; rather it exhibits distortion in the form of an asymmetry between negative and positive velocities.

The spectrogram of the velocity response [Fig. 1(b)] shows the time behavior of the spectral content in the velocity time waveform. As the acoustic intensity of the stimulus increases towards the center of the envelope, multiple harmonic components are generated. The component at $2f_c$ is first to appear (at 0.09 s), followed in time by $3f_c, 4f_c$, and $5f_c$. More harmonic components may be present, but the sampling rate of the data collection does not permit them to be viewed.

Figure 1(c) provides a different view on the spectrogram. It explicitly shows the time variation of the four most significant spectral components, at $f_c, 2f_c, 3f_c$, and $4f_c$. The plot is symmetrical in time about the center of the modulation envelope. The component at $2f_c$ is seen to appear before the component at $3f_c$ but their magnitudes are approximately equal for the time range 0.17–0.25 s near the center of the envelope.

4.2 Response of an outer hair cell to an AM stimulus with a carrier frequency at its characteristic frequency

Figure 2(a) shows the velocity response of the same cell to an AM stimulus with $f_c = 706$ Hz (at CF). Comparison with Fig. 1(a) shows that the peak velocity is higher by about a factor of 10 for the same sound pressure level.

The spectrogram of the velocity response [Fig. 2(b)] demonstrates the presence of three principal spectral components: $f_c, 2f_c$, and $3f_c$. Near the center of the envelope, the component at $3f_c$ is clearly dominant with respect to that at $2f_c$.

Figure 2(c) shows that the responses at the carrier frequency and at the harmonics do not follow the envelope of the modulating signal. There is a slight asymmetry in time about the center of the modulating envelope (at .205 s), with the third harmonic not reaching a peak until 0.28 s. The response is therefore not simply a function of the instantaneous input stimulus but it also depends on past history. Note also that the component at $3f_c$ starts later, and finishes earlier, in time than the component at $2f_c$, yet it is far more significant in the response at the higher sound pressure levels, indicating that the spectrum of the response is level dependent. Since these cells also undergo displacement shifts in response to AM stimuli (Brundin *et al.*, 1991; Brundin *et al.*, 1992), the asymmetry in time may reflect an underlying change in the dynamical response due to the positional change of the cell.

4.3 Response of an outer hair cell to an AM stimulus with a carrier frequency above its characteristic frequency

Figure 3(a) shows the velocity response of the same cell to an AM stimulus with $f_c = 1013$ Hz (above CF). The magnitude of the velocity waveform is lower than

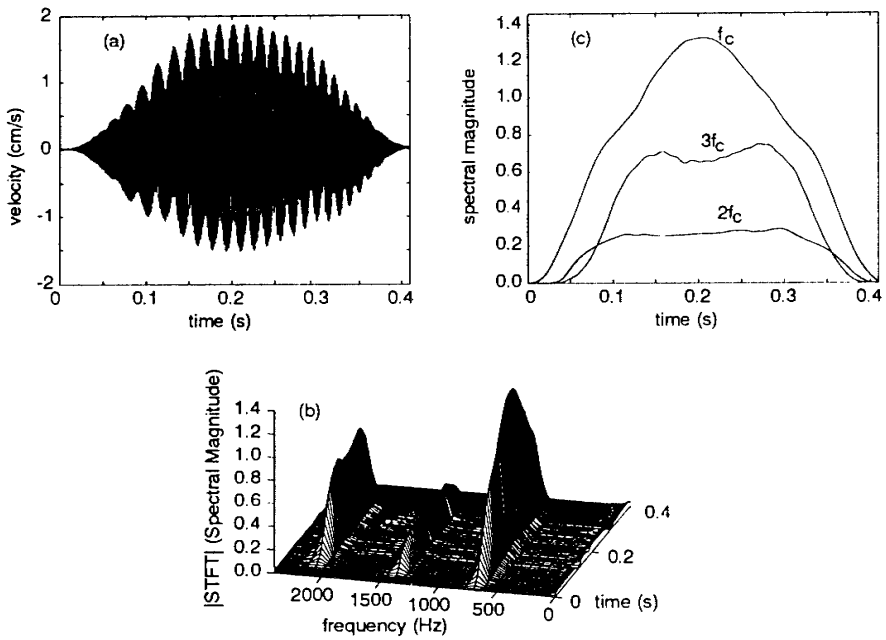

Figure 2: Velocity response of the same outer hair cell as in Fig. 1, but now to an AM stimulus with f_c = 706 Hz (at CF) and a modulation frequency of 2.44 Hz. (*a*) Time waveform of the velocity response (in cm/s). Though the sound pressure level is the same as that for Fig. 1, the velocity response is considerably enhanced in magnitude since the carrier frequency is near the CF of the cell. The "scalloping" apparent on the envelope of the raw data arises from false modulation and disappears with correct digital-signal interpolation. (*b*) Spectrogram of the velocity response shown in (*a*). The spectrogram has components at the carrier frequency f_c and at the harmonics $2f_c$ and $3f_c$. The component at $3f_c$ is almost three times greater in magnitude than the component at $2f_c$ near the center of the modulation envelope. (*c*) Time course of the three largest spectral components in the velocity response ($f_c, 2f_c$, and $3f_c$), extracted directly from the spectrogram in (*b*). The magnitudes of the spectral components are no longer precisely symmetrical functions of time with respect to the center of the modulation envelope; the spectral component at $3f_c$ does not reach a peak until 0.28 s.

its value at CF. The envelope of the response follows the stimulus envelope with no distortion (again the "scalloping" on this raw data carries no information).

The spectrogram of the velocity response [Fig. 3(b)] indicates a component at the carrier frequency and at its first harmonic. It is not possible to investigate the presence of a response at $3f_c$ since components at that frequency was removed by anti-aliasing filters in the experiment prior to sampling. The two spectral components are

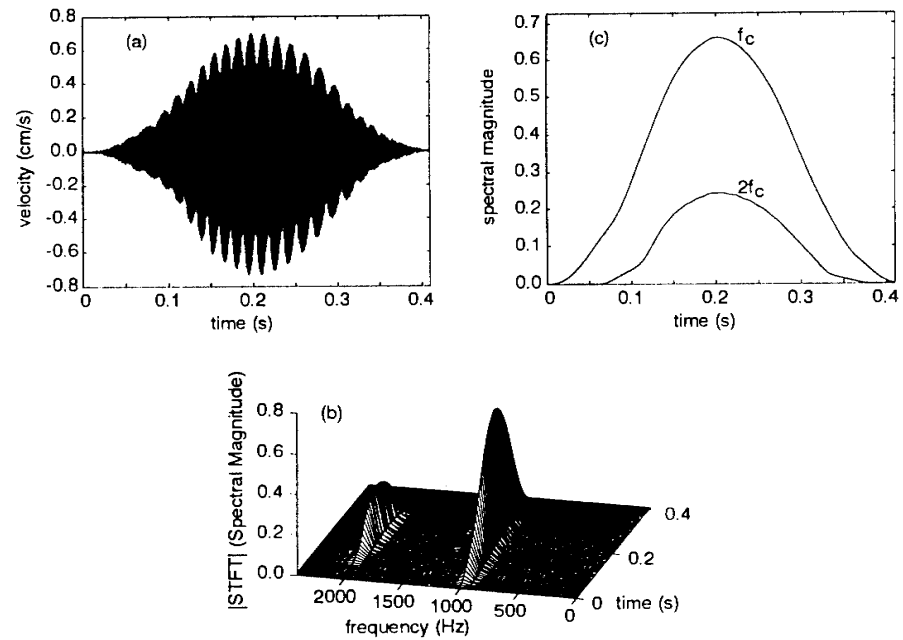

Figure 3: Velocity response of the same outer hair cell as in Figs. 1 and 2 to an AM stimulus with f_c = 1013 Hz (above CF) and a modulation frequency of 2.44 Hz. (*a*) Time waveform of the velocity response (in cm/s). (*b*) Spectrogram of the velocity response shown in (*a*). (*c*) Time course of the two spectral components present in the velocity response, extracted directly from the spectrogram in (*b*). The magnitude of the spectral components are again symmetrical functions of time with respect to the center of the modulation envelope.

symmetrical in time with respect to the center of the modulation envelope [Fig. 3(c)].

5 Discussion

The use of a slowly varying AM stimulus with a range of carrier frequencies, allows us to clearly examine the level-dependent and frequency-dependent nonlinear dynamics in the responses of outer hair cells and Hensen's cells. The results presented here are typical of the 34 data sets we investigated, taken from 8 outer hair cells and 8 Hensen's cells from 7 different animals. Analysis of the velocity response waveforms using the spectrogram has shown the following:

(i) The nonlinearity of the dynamics increases with sound pressure level. This is evident in the spectrograms, where the generation of harmonics (a nonlinear effect) sets in at higher sound pressure levels (away from the edges of the envelope).

(ii) The patterns of harmonic generation for AM stimuli of a given peak sound pressure

level depend upon the carrier frequency of the stimulus relative to the CF of the cell. As an example, the spectral component at $3f_c$ is greater than that at $2f_c$ for carrier frequencies near CF, but these components are approximately equal in magnitude below CF. At higher sound pressure levels than those illustrated here, half-harmonic as well as harmonic components also appear.
(iii) The cellular reponse is not simply a function of instantaneous input, but it depends on prior events also. By tracing the time-varying spectrum of the response, we observe that precisely the same stimulus level produces differing spectral responses depending upon prior input.

In short, we have found that the spectrogram is a valuable tool for qualitatively and quantitatively analyzing the time-varying nonlinear responses of cellular structures in the organ of Corti. This analysis tool provides important information for modeling the response of these cellular structures, since it summarizes the frequency-dependent and level-dependent behavior of various elements in these structures in a single picture.

6 Acknowledgments

This research was supported by the Office of Naval Research under Grant N00014-92-J-1251, by the National Institutes of Health through NIDCD Program Project Grant DC00316, by the Emil Capita Foundation, by the Swedish Medical Research Council (02461), by the Magnus Bergvall Foundation, and by the Tysta Skolan Foundation.

References

Brundin, L., Flock, Å., Khanna, S. M., and Ulfendahl, M. (**1991**). "Frequency specific shift of the guinea pig organ of Corti", Neurosci. Lett., **128**, 77–86.

Brundin, L., Flock, Å., Khanna, S. M., and Ulfendahl, M. (**1992**). "The tuned displacement response of the hearing organ is generated by the outer hair cells", Neuroscience **49**, 607–616.

Franke, R., Dancer, A., Khanna, S. M., and Ulfendahl, M. (**1992**). "Intracochlear and extracochlear pressure measurements in the temporal bone preparation of the guinea pig", Acustica **76**, 173–182.

ITER (International Team for Ear Research) (**1989**). "Cellular vibration and motility in the organ of Corti", Acta Otolaryngol. (Stockholm) Suppl. **467**, 1–279.

LePage, E. and Johnstone, B. M. (**1980**). "Nonlinear mechanical behavior of the basilar membrane in the basal turn of the guinea pig cochlea", Hear. Res. **2**, 183–189.

Oppenheim, A. V. and Schafer, R. W. (**1989**). *Discrete-Time Signal Processing* (Prentice Hall, Englewood Cliffs, NJ), pp. 713–726.

Rhode, W. S. (**1971**). "Observations of the vibration of basilar membrane in squirrel monkeys using the Mössbauer technique", J. Acoust. Soc. Am. **49**, 1218–1231.

Robles, L., Ruggero, M. A., and Rich, N. C. (**1989**). "Nonlinear interactions in the mechanical response of the cochlea to two-tone stimuli", in *Cochlear Mechanisms - Structure, Function and Models*, edited by J. P. Wilson and D. T. Kemp (Plenum, London), pp. 369–375.

Sellick, P. M., Yates, G. K., and Patuzzi, R. (**1982**). "Measurement of basilar membrane motion in the guinea pig using the Mössbauer technique", J. Acoust. Soc. Am. **72**, 131–141.

Teich, M. C., Khanna, S. M., and Keilson, S. E. (**1989**). "Nonlinear dynamics of cellular vibrations in the organ of Corti", Acta Otolaryngol. (Stockholm) Suppl. **467**, 265–279.

Ulfendahl, M., Flock, Å., and Khanna, S. M. (**1989**). "A temporal bone preparation for the study of cochlear micromechanics at the cellular level", Hear. Res. **40**, 55–64.